Isolation and Characterization of Cellulose Nanofibers from *Bambusa rigida*

Wen He,* Shenxue Jiang, Qisheng Zhang, and Minzhu Pan

Alpha cellulose was extracted from *Bambusa rigida* fibers by carrying out Soxhlet extraction and bleaching and alkali treatments with acidified sodium chlorite solution and sodium hydrate solution. Then, cellulose nanofibers were isolated from α-cellulose with the combination of (33 wt%) sulfuric acid and ultrasonic treatment. The nano-sized fibers were successfully isolated, and the average diameters were about 10 to 30 nm. FTIR showed that a majority of the hemicelluloses and lignin were removed from the raw fiber and that the chemical constituents of α-cellulose and cellulose nanofibers were similar. XRD showed that the obtained nano-fibers presented a cellulose I structure, and thus the crystallinity of cellulose nanofibers was significantly increased. TGA showed that the thermal stability of the cellulose nanofibers was significantly improved. The relative crystallinity and thermal degradation temperature of the cellulose nanofibers reached 61.21% and 315.2 ^{o}C, respectively.

Keywords: Bambusa rigida; α-Cellulose; Cellulose nanofiber; Thermal properties; X-ray diffraction (XRD)

*Contact information: Bamboo Engineering Research Center, Nanjing Forestry University, Nanjing 210037, China; *Corresponding author: hewen2011@njfu.edu.cn*

INTRODUCTION

In recent decades, cellulose nanofibers have attracted extensive interest because of their negligible thermal expansion, superior mechanical properties, high surface area-to-volume ratio, and high surface area, as well as their sustainability, biocompatibility, and broad chemical modification and assembly capacity (Beecher 2007; Dong *et al*. 2012; Habibi *et al*. 2010; Nakagaito *et al*. 2010). Today, applications of cellulose nanofibers are focused on numerous areas: biomedical applications (Czaja *et al*. 2007; Klemm *et al*. 2005), reinforcement in nanocomposites (Nogi and Yano 2008; Wu *et al.* 2012), electronic papers and fuel cell membranes (Shah and Brown 2004; Shi *et al*. 2012), gas barrier films and optically transparent functional materials (Fukuzumi *et al*. 2009; Liu and Berglund 2012; Nogi *et al*. 2009), among others.

In general, cellulose nanofibers are isolated from a number of different cellulosic sources, such as natural plant fibers, algae, tunicates, and bacterial cellulose. As an important natural resource, wood is widely used to isolate cellulose nanofibers; however, the demand for such raw materials has increased. Therefore, interest in agricultural crops and their by-products, such as sugar beet pulp (Habibi and Vignon 2007), wheat straw and soy hulls (Alemdar and Sain 2008), or even bagasse (Bhattacharya *et al*. 2008), palm trees (Bendahou *et al*. 2010), ramie (Bhattacharya *et al*. 2008), carrots (Siqueira *et al*. 2010a), and bamboo (Chen *et al*. 2011), is increasing. It has become important to find renewable plants for use in the production industries.

A number of isolation methods have been used to disintegrate cellulose nanofibers from various cellulosic materials. The main methods have been based on mechanical treatments, including homogenizing and microfluidizing (Aulin 2009; Dinand *et al*. 2002), grinding (Iwamoto *et al*. 2007), and cryocrushing (Alemdar *et al*. 2008). In general, pre-treatments have been applied prior to the mechanical process, including sulfuric acid hydrolysis (Elazzouzi-Hafraoui *et al*. 2007), hydrochloric acid hydrolysis (Araki *et al*. 2000; Ummartyotin *et al*. 2012), TEMPO-mediated oxidation (Saito and Isogai 2006), carboxymethylation (Aulin *et al*. 2009), and enzyme-assisted hydrolysis (Pääkkö *et al*. 2007). Generally speaking, all these methods lead to different types of nanofibrillar materials, depending on the cellulose raw material, its pretreatment, and the disintegration process itself.

Recently, the combination of sulfuric acid and ultrasonication to isolate cellulose nanofibers has been reported by some researchers. The methods proposed were convenient and had less effect on the fiber characteristics and properties (Cheng *et al*. 2007; Tischer *et al*. 2010). Sulfuric acid hydrolysis mainly removes the amorphous regions of the cellulose, leaving the crystalline regions in a stable colloidal suspension due to the electrostatic repulsion between the negative sulfate groups on the cellulose microfibril surface (Siqueira *et al*. 2010b). During an ultrasonic treatment, strong mechanical oscillating powers generally break down the interaction force between cellulose microfibrils and finally disintegrate the fibers into nanofibers.

Bambusa rigida is a medium-sized sympodial bamboo, which is a fast-growing plant and contains abundant celluloses. Generally, it is used to manufacture handles for farm tools and bamboo plywood, therefore, *Bambusa rigida* has lower economic values. However, the isolation and characterization of cellulose nanofibers from *Bambusa rigida* has not been previously reported. This study was designed to isolate cellulose nanofibers from *Bambusa rigida* fibers using a combination of sulfuric acid treatment and an ultrasonic process. The morphology, crystallinity, and thermal properties of the isolated nanofibers and their intermediate products were characterized by scanning electron microscopy (SEM), transmission electron microscopy (TEM), Fourier transform infrared spectros-copy (FTIR), X-ray diffraction (XRD), and thermogravimetric analysis (TGA).

EXPERIMENTAL

Raw Materials Preparation

Bambusa rigida was collected from a bamboo plantation in Nanjing county in Jiangsu province, China (31°14'N to 32°36'N, 118°22'E to 119°14'E). Both the outer and inner sides of bamboo culms were removed. The remaining part was cut into small pieces and then ground into powder (using 60 to 80 mesh) as original material, and then the powder was oven-dried at 105 °C for 24 h and stored in a desiccator at room temperature. Benzene, ethanol, sodium chlorite, acetic acid, potassium hydroxide, sulfuric acid, and other chemicals were of laboratory grade and were used without further purification.

Extraction of α-cellulose

The extraction of α-cellulose from *B. rigida* was performed according to the methods of Abe *et al*. (2007) and Abe and Yano (2009). Bamboo powders were first dewaxed in a Soxhlet apparatus with a 2:1 (v/v) mixture of benzene and ethanol for 6 h to remove part of the extractives, and then the dewaxed sample was washed with neutral tap

water and dried for 12 h at 100 °C in an air-circulating oven. Lignin in the dewaxed sample was then removed using an acidified sodium chlorite solution at 70 °C for 1 h, and the process was repeated six times; then, the product was washed with distilled water until it became neutral. Next, the product was soaked in a 5 wt% potassium hydroxide solution for 24 h and vigorously stirred at 90 °C for 2 h to remove hemicelluloses, residual starch, and pectin. After these chemical treatments, the product was filtered and cleaned with distilled water until it was neutral.

Isolation of Cellulose Nanofibers

Cellulose nanofibers were prepared by the combination of acid hydrolysis and ultrasonic treatment from the cellulose obtained above. Acid hydrolysis was carried out using a 33 wt% sulfuric acid solution at 90 °C. The time of hydrolysis in this study was fixed at 60 min, which was found to be the optimum time. The ratio of the obtained cellulose to distilled water was 1:10 (wt%). Once the reaction time was reached, distilled water of about 20 ^{o}C was added to stop the reaction. The sulfuric acid was partially removed from the resulting suspension by centrifugation (10,000 rpm, 10 min). The un-reactive sulfate groups were removed by centrifugation following dialysis. Then, the samples were resuspended and dialyzed against distilled water with a cellulose membrane until the pH reached 7. Next, the resulting cellulose was diluted in distilled water (0.1% by mass), and the suspension obtained was then sonicated for 20 min using an ultrasonic processor (JY98-IIID, Ningbo Scientz Biotechnology, China) at 15 to 20 kHz and an output power of 800 W to isolate the nanofibers. The ultrasonic treatment was carried out in an ice bath; the ice was maintained throughout the entire ultrasonication.

Scanning Electron Microscopy (SEM)

Suspensions of the cellulose fibers after the ultrasonic process were subjected to freeze-drying. The obtained sheets were coated with gold by an ion sputter coater and were observed under a scanning electron microscope (JSM-7600F, Japan) operating at 12.5 and 20 kV.

Transmission Electron Microscopy (TEM)

TEM observation of the resultant suspension of cellulose nanofibers was performed on a JEM-2100 (Japan) electron microscope at an acceleration voltage of 80 kV. The diluted cellulose nanofibers were dropped onto carbon-coated electron microscopy grids and then negatively stained by 1% phosphotungstic acid solution. A TDY-V5.2 microscope image analysis system was used to measure the diameter of cellulose nanofibers from the TEM images. The dimensional quantities were calculated from the measurement of dozens of nanofibers and used to analyze the diameter distribution.

Fourier Transform Infrared (FTIR) Spectroscopy

FTIR spectra were recorded on a Fourier transform infrared (FTIR) instrument (Nicolet Magna 560, USA) in the range of 600 to 4000 cm^{-1} with a resolution of 4 cm^{-1}. The samples were ground into powder by a fiber microtome and then blended with KBr before the mixture was pressed into ultra-thin pellets.

X-ray Diffraction (XRD) Analysis

The X-ray diffraction (XRD) patterns of the original bamboo fiber, holo-cellulose, α-cellulose, and isolated cellulose nanofibers were obtained with an X-ray diffractometer (D/max 2200, Rigaku, Japan) using Ni-filtered CuKa radiation (k = 1.5406 Å) at 40 kV and 30 mA. Scattered radiation was detected in the range of 2θ = 10 to 30° at a scan rate of 4°/min. The crystallinity index (C_I) was calculated from the height of the 200 peak (I_{200}, 2h = 22.6°) and the intensity minimum between the 200 and 110 peaks (I_{am}, 2h = 18°) using the Segal method (Segal and Meshulam 1979), as shown in Eq. 1. I_{200} represents both crystalline and amorphous material,

$$C_I(\%) = \left(1 - \frac{I_{am}}{I_{200}}\right) \times 100 \quad (1)$$

where I_{am} represents the amorphous material.

Thermogravimetric Analysis (TGA)

Thermogravimetric analysis (TGA) was performed using a thermogravimetric analyzer (Pyris 6, Perkin-Elmer, USA) to determine the thermal stability of cellulose fibers at different stages of purification. The samples were heated from room temperature to 600 °C under a nitrogen atmosphere at a heating rate of 10 °C/min.

RESULTS AND DISCUSSION

Morphological Analysis

Figure 1 shows SEM images of the intermediate products during disintegration of cellulose nanofibers. The aliphatic acid, pigment, and other extracts were removed from the raw material after Soxhlet extraction with a mixture of benzene and ethanol, and the color of the raw fiber became light yellow.

Figures 1c and 1d show the morphology of holo-cellulose and α-cellulose, respectively. It is apparent that after the chemical treatments, the raw fibers were separated into individual micro-sized fibers, which were reported to be composed of strong hydrogen bonding nanofibers (Abe and Yano 2009, 2010). On the other hand, it can be shown that the α-cellulose was separated into two distinguishably different types of cells, fibrous cells and rectangular cells, which can be regarded as fiber and parenchyma cells, respectively (Abe and Yano 2010).

Figure 1e and Fig. 2 show the morphology of cellulose nanofibers under SEM and TEM, respectively. Both figures display a classical web-like network structure in which the fibers occur as very long entangled cellulosic filaments. Figure 3 shows the diameter range of cellulose nanofibers obtained: The lateral size of cellulose nanofibers was about 10 to 30 nm in width.

Generally, the diameter of a single microfibril is reported to be about 3 to 5 nm in higher plants (Somerville *et al*. 2004). Hence, the observed nanofiber is suggested to be the original fibril aggregates. This finding indicates that fine nanofibers were successfully obtained from *Bambusa rigida*.

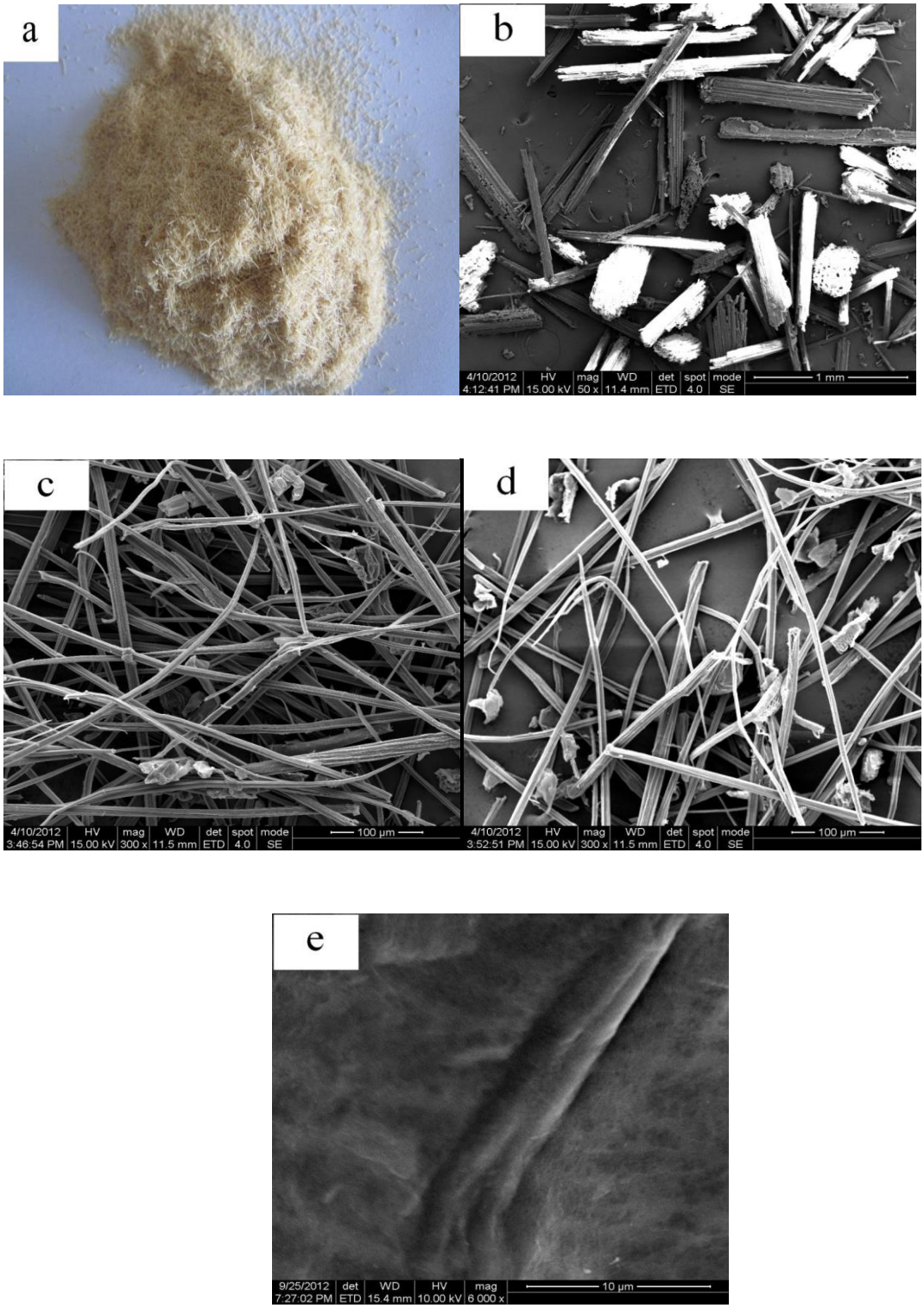

Fig. 1. Photograph (a) raw fiber and SEM images of (b) extracted fiber, (c) holo-cellulose, (d) α-cellulose, and (e) cellulose nanofibers

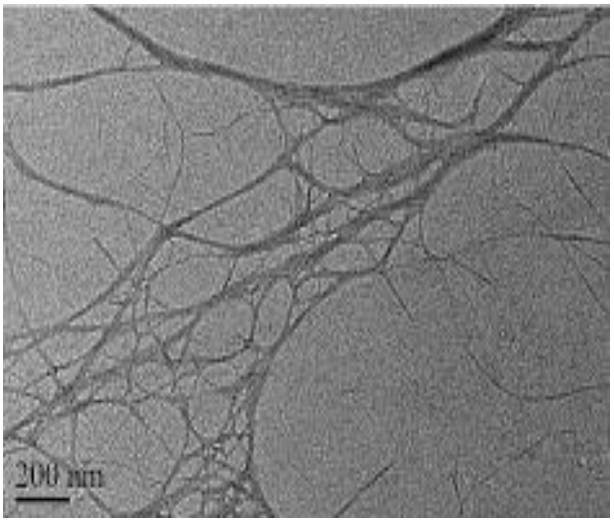

Fig. 2. TEM image of cellulose nanofibers

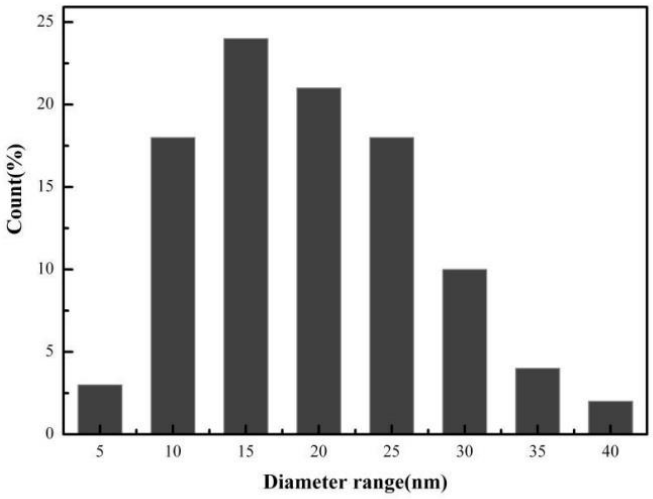

Fig. 3. Diameter range of cellulose nanofibers

FTIR Spectroscopy Analysis

FTIR spectra of the cellulose nanofibers and their intermediate products are shown in Fig. 4. The peak at 1510 cm^{-1} in the spectrum of the original fiber, which is attributed to the C=C stretching vibration in the aromatic ring of lignin (Sun *et al*. 2000; Juby *et al*. 2012), disappeared completely on the curve of holo-cellulose. This indicates that lignin was well removed from the newly prepared holo-cellulose by acidic $NaClO_2$ treatment. The peak at 1733 cm^{-1} in the spectrum of holo-cellulose represents either the acetyl and uronic ester groups or the ester linkage of the carboxylic group of the ferulic and p-coumeric acids of the hemicelluloses (Sain and Panthapulakkal 2006; Juby *et al.* 2012). However, this peak disappeared completely in the spectra of α-cellulose and cellulose nanofibers, which could be attributed to the removal of most of the hemicelluloses after KOH treatment. On the other hand, after sulfuric acid and ultrasonic treatment, the spectrum of the cellulose nanofibers was fairly close to that of the α-cellulose.

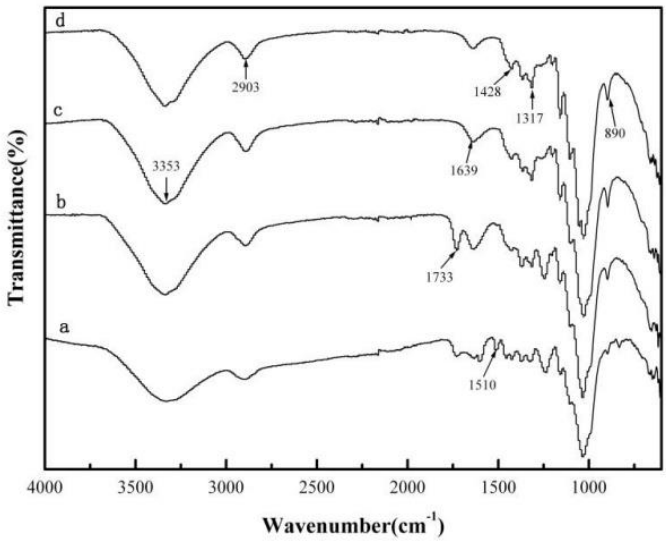

Fig. 4. FTIR spectra of cellulose nanofibers isolated in all stages: (a) raw material, (b) holo-cellulose, (c) α-cellulose, and (d) cellulose nanofibers

The band at 3353 cm^{-1} is attributed to the O–H stretching vibration. The bands at 2903 and 1428 cm^{-1} are characteristics of C–H stretching and bending of $–CH_2$ groups, respectively, whereas the peaks at 1639 and 890 cm^{-1} are attributed to the H–O–H stretching vibration of absorbed water in carbohydrates and the C_1-H deformation vibrations of cellulose, respectively. This fact indicated that hemicelluloses and lignin were to a large degree removed after chemical purification and that the original molecular structure of the cellulose was maintained even after the removal of the matrix components and after ultrasonic treatments.

XRD Analysis

XRD analysis was performed to investigate the crystalline behavior of the cellulose fibers. Figure 5 and Table 1 show the corresponding X-ray diffraction patterns and the relative degree of crystallinity of the raw material, holo-cellulose, α-cellulose, and cellulose nanofibers. All the diffractograms show peaks at around 2θ = 16.5° and 22.5°, which are believed to represent the typical cellulose I structure, indicating that the crystal integrity had been maintained (Nishiyama *et al*. 2002, 2003). The relative degree of crystallinity in the raw fiber, holo-cellulose, and α-cellulose was 52.50%, 54.24%, and 59.47%, respectively. Obviously, the crystallinity of celluloses increased after chemical treatment, which can be attributed to the removal of lignin and hemicelluloses present in the amorphous regions. In addition, the crystallinity of cellulose nanofibers had a slight increase, with a value of about 61.21%, which could be a result of the damage to the amorphous regions of α-cellulose after being treated with sulfuric acid. The highly crystalline nanofibers could be more effective in providing better reinforcement and thermal stability for composite materials.

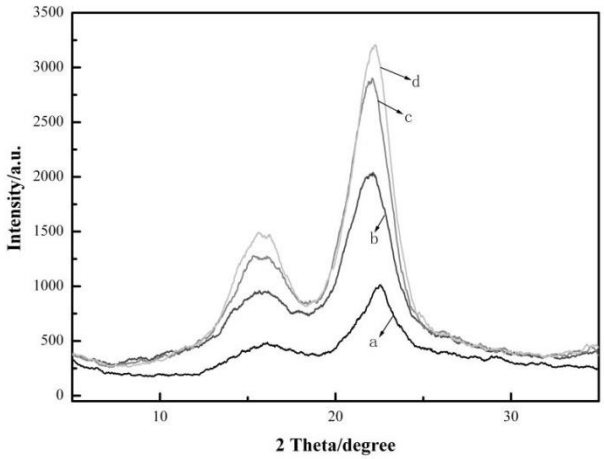

Fig. 5. X-ray diffraction patterns of (a) raw material, (b) holo-cellulose, (c) α-cellulose, and (d) cellulose nanofibers

Table 1. Crystallinity of Cellulose Fibers at Different Stages

Samples	Relative Crystallinity (%)
Raw fiber	52.50
Holo-cellulose	54.24
α-cellulose	59.47
Cellulose nanofiber	61.21

Thermal Stability Analysis

Figure 6 shows thermogravimetric curves of the raw material, chemically-treated cellulose fibers, and cellulose nanofibers.

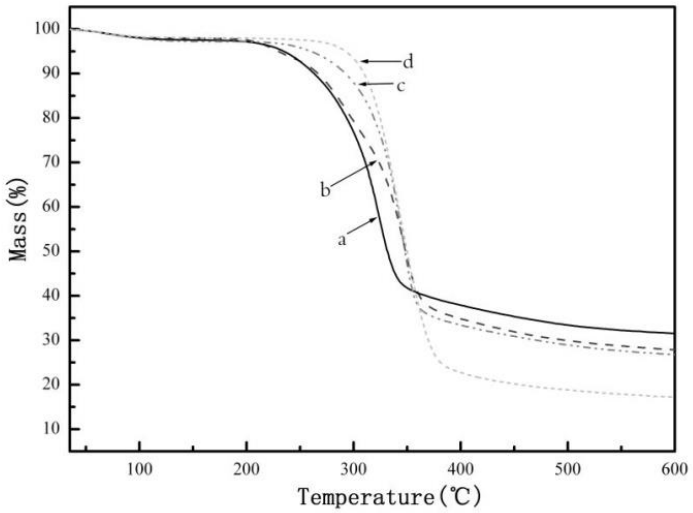

Fig. 6. TG curves of (a) raw material, (b) holo-cellulose, (c) α-cellulose, and (d) cellulose nanofibers

All the TG curves showed an initial small mass loss around 100 °C, which could be attributed to the evaporation of absorbed moisture (approximately 5%). The curves of the raw material and holo-cellulose showed several different decomposition stages, which indicate the presence of different components. The raw material showed a lower original decomposition temperature (about 223 ^{o}C) due to the presence of hemicelluloses and lignin (Wielage *et al.* 1999). The original degradation temperature of holo-cellulose slightly increased to 231 ^{o}C due to the removal of lignin. Apparently, the degradation temperature of α-cellulose was increased to 308.5 ^{o}C due to the removal of hemicelluloses and lignin after chemical extraction. For the cellulose nanofibers, the decomposition temperature increased to 315.2 ^{o}C, which could be due to the removal of the alkali-insoluble matrix existing in the α-cellulose after being treated with sulfuric acid. These findings are in accordance with the results obtained from FTIR and X-ray measurements. The higher thermal stability of the cellulose nanofibers compared with the raw material may broaden the application area of cellulose fibers, especially at temperatures higher than 200 ^{o}C, for biocomposite processing.

CONCLUSIONS

1. Cellulose nanofibers were isolated from *Bambusa rigida* by chemical treatments followed by ultrasonic fibrillation. Nanofibers with diameters ranging from 10 to 30 nm were successfully isolated from the raw material.
2. FTIR measurements of the fibers revealed the complete removal of hemicelluloses and lignin during the chemical process.
3. The degree of crystallinity of the cellulose nanofibers reached was about 60.8%, and cellulose nanofibers presented a typical cellulose I structure.
4. The cellulose nanofibers also exhibited enhanced thermal properties, with a thermal degradation temperature higher than 315 ^{o}C, compared with that of approximately 220 ^{o}C for the raw material.

ACKNOWLEDGMENTS

This work was financially supported by the High-level Talent Fund of Nanjing Forestry University (Fund Number 013020186) and a Project Funded by the Priority Academic Program Development of Jiangsu Higher Education Institutions (PAPD). The authors would like to acknowledge the support of Dr. Yihu Wang. Thanks go also to Ms. Wenli Chen for TEM operation.

REFERENCES CITED

Abe, K., and Yano, H. (2009). "Comparison of the characteristics of cellulose microfibril aggregates of wood, rice straw and potato tuber," *Cellulose* 16(6), 1017-1023.

Abe, K., and Yano, H. (2010). "Comparison of the characteristics of cellulose microfibril aggregates isolated from fiber and parenchyma cells of Moso bamboo (*Phyllostachys pubescens*)," *Cellulose* 17(2), 271-277.

Abe, K., Iwamoto, S., and Yano, H. (2007). "Obtaining cellulose nanofibers with a uniform width of 15 nm from wood," *Biomacromol*. 8(10), 3276-3278.

Alemdar, A., and Sain, M. (2008). "Isolation and characterization of nanofibers from agricultural residues—Wheat straw and soy hulls," *Bioresource Technology* 99(6), 1664-1671.

Araki, J., Wada, M., Kuga, S., and Okano, T. (2000). "Birefringent glassy phase of a cellulose microcrystal suspension," *Langmuir* 16(6), 2413-2415.

Aulin, C. (2009). *Novel Oil Resistant Cellulosic Materials (Pulp and Paper Technology)*, Stockholm: KTH Chemical Science and Engineering.

Aulin, C., Ahola, S., Josefsson, P., Nishino, T., Hirose, Y., Osterberg, M., and Wågberg, L. (2009). "Nanoscale cellulose films with different crystallinities and mesostructures—Their surface properties and interaction with water," *Langmuir* 25(13), 7675-7685.

Beecher, J. F. (2007). "Organic materials: Wood, trees and nanotechnology," *Nat. Nanotechnol*. 2(8), 466-467.

Bendahou, A., Kaddami, H., and Dufresne, A. (2010). "Investigation on the effect of cellulosic nanoparticles' morphology on the properties of natural rubber based nanocomposites," *European Polymer Journal* 46(4), 609-620.

Bhattacharya, D., Germinario, L. T., and Winter, W. T. (2008). "Isolation, preparation and characterization of cellulose microfibers obtained from bagasse," *Carbohydrate Polymers* 73(3), 371-377.

Chen, W. S., Yu, H. P., Liu, Y. X., Chen, P., Zhang, M. X., and Hai, Y. F. (2011). "Individualization of cellulose nanofibers from wood using high-intensity ultrasonication combined with chemical pretreatments," *Carbohydr Polym*. 83(4), 1804-1811.

Cheng, Q., Wang, S., Rials, T., and Lee, S. (2007). "Physical and mechanical properties of polyvinyl alcohol and polypropylene composite materials reinforced with fibril aggregates isolated from regenerated cellulose fibers," *Cellulose* 14(6), 593-602.

Czaja, W., Krystynowicz, A., Kawecki, M., Wysota, K., Sakiel, S., and Wroblewski, P. (2007). "Biomedical applications of microbial cellulose in burn wound recovery," *Cellulose: Molecular and Structural Biology: Selected Articles on the Synthesis, Structure and Applications of Cellulose* 8(2), 307-321.

Dinand, E., Maureaux, A., Chanzy, H., Vincent, I., and Vignon, M. R. (2002). "Microfibrillated cellulose and process for making the same from vegetable pulps having primary walls, especially from sugar beet pulp," Patent # EP 0726356 B1.

Dong, H., Strawhecker, K. E., Snyder, J. F., Orlicki, J. A., Reiner, R. S., and Rudie, A.W. (2012). "Cellulose nanocrystals as a reinforcing material for electrospun poly(methyl methacrylate) fibers: Formation, properties and nanomechanical characterization," *Carbohydrate Polymers* 87(4), 2488-2495.

Elazzouzi-Hafraoui, S., Nishiyama, Y., Putaux, J. L., Heux, L., Dubreuil, F., and Rochas, C. (2007). "The shape and size distribution of crystalline nanoparticles prepared by acid hydrolysis of native cellulose," *Biomacromol.* 9(1), 57-65.

Fukuzumi, H., Saito, T., Iwata, T., Kumamoto, Y., and Isogai, A. (2009). "Transparent and high gas barrier films of cellulose nanofibers prepared by TEMPO-mediated oxidation," *Biomacromolecules* 10(1), 162-165.

Habibi, Y., and Vignon, M. R. (2007). "Optimization of cellouronic acid synthesis by TEMPO-mediated oxidation of cellulose III from sugar beet pulp," *Cellulose* 15(1), 177-185.

Habibi, Y., Lucia, L. A., and Rojas, O. J. (2010). "Cellulose nanocrystals: Chemistry, self-assembly, and applications," *Chem. Rev*. 110(6), 3479-3500.

Iwamoto, S., Nakagaito, A. N., and Yano, H. (2007). "Nano-fibrillation of pulp fibers for the processing of transparent nanocomposites," *Applied Physics A* 89(2), 461-466.

Juby, K. A., Dwivedi, C., Kumar, M., Swathi, K., Misra, H. S., and Bajaj, P. N. (2012). "Silver nanoparticle-loaded PVA/gum acacia hydrogel: Synthesis, characterization and antibacterial study," *Carbohydrate Polymers* 89, 906-913.

Klemm, D., Heublein, B., Fink, H.-P., and Bohn, A. (2005). "Cellulose: Fascinating biopolymer and sustainable raw material," *Angewandte Chemie International Edition* 44(22), 3358-3393.

Liu, A. D., and Berglund, L. A. (2012). "Clay nanopaper composites of nacre-like structure based on montmorrilonite and cellulose nanofibers. Improvements due to chitosan addition," *Carbohydr Polym*. 87, 53-60.

Nakagaito, A., Mangalam, A., Simonsen, J., Benight, A., Bismarck, A., Berglund, L., and Peijs, T. (2010). "Review: Current international research into cellulose nanofibres and nanocomposites," *J. Mater. Sci*. 45(1), 1-33.

Nishiyama, Y., Langan, P., and Chanzy, H. (2002). "Crystal structure and hydrogen-bonding system in cellulose Ib from synchrotron X-ray and neutron fiber diffraction," *J. Amer. Chem. Soc*. 124, 9074-9082.

Nishiyama, Y., Sugiyama, J., Chanzy, H., and Langan, P. (2003). "Crystal structure and hydrogen bonding system in cellulose Iα from synchrotron X-ray and neutron fiber diffraction," *J. Amer. Chem. Soc*. 125(47), 14300–14306.

Nogi, M., and Yano, H. (2008). "Transparent nanocomposites based on cellulose produced by bacteria offer potential innovation in the electronics device industry," *Advanced Materials* 20(10), 1849-1852.

Nogi, M., Iwamoto, S., Nakagaito, A. N., and Yano, H. (2009). "Optically transparent nanofiber paper," *Advanced Materials* 21(16), 1595-1598.

Pääkkö, M., Ankerfors, M., Kosonen, H., Nykanen, A., Ahola, S., Osterberg, M., Ruokolainen, J., Laine, J., Larsson, P. T., Ikkala, O., and Lindström, T. (2007). "Enzymatic hydrolysis combined with mechanical shearing and high-pressure homogenization for nanoscale cellulose fibrils and strong gels," *Biomacromolecules* 8(6), 1934-1941.

Sain, M., and Panthapulakkal, S. (2006). "Bioprocess preparation of wheat straw fibers and their characterization," *Ind. Crops Prod*. 23(1), 1-8.

Saito, T., and Isogai, A. (2006). "Introduction of aldehyde groups on surfaces of native cellulose fibers by TEMPO-mediated oxidation," *Colloids and Surfaces A* 289, 219-225.

Segal, A. W., and Meshulam, T. (1979). "Production of superoxide by neutrophils: A reappraisal," *FEBS Lett.* 100(1), 27-32.

Shah, J., and Brown, R. M. (2004). "Towards electronic paper displays made from microbial cellulose," *Applied Microbiology and Biotechnology* 66(4), 352-355.

Shi, Q., Zhou, C., Yue, Y., Guo, W., Wu, Y., and Wu, Q. (2012). "Mechanical properties and in vitro degradation of electrospun bio-nanocomposite mats from PLA and cellulose nanocrystals," *Carbohydr. Polym*. 90(1), 301-308.

Siqueira, G., Tadokoro, S. K., Mathew, A. P., and Oksman, K. (2010a). "Carrot nanofibers and nanocomposites applications," presented at the 7th International Symposium on Natural Polymers and Composites, Gramado, Brazil; September 7-10, 2010.

Siqueira, G., Tapin-Lingua, S., Bras, J., Da Silva Perez, D., and Dufresne, A. (2010b). "Morphological investigation of nanoparticles obtained from combined mechanical shearing, and enzymatic and acid hydrolysis of sisal fibers," *Cellulose* 17(6), 1147-1158.

Somerville, C., Bauer, S., Brininstool, G., Facette, M., Hamann, T., Milne, J., Osborne, E., Paredez, A., Persson, S., Raab, T., Vorwerk, S., and Youngs, H. (2004). "Toward a systems approach to understanding plant cell walls," *Science* 306(5705), 2206-2211.

Tischer, P. C. S. F., Sierakowski, M. R., Westfahl, H., and Tischer, C. A. (2010). "Nanostructural reorganization of bacterial cellulose by ultrasonic treatment," *Biomacromol*. 11(5), 1217-1224.

Ummartyotin, S., Juntaro, J., Sain, M., and Manuspiya, H. (2012). "Development of transparent bacterial cellulose nanocomposite film as substrate for flexible organic light emitting diode (OLED) display," *Indus. Crop. Prod*. 35, 92-97.

Wielage, B., Lampke, G., Marx, K., and Nestler, D. (1999). "Thermogravimetric and differential scanning calorimetric analysis of natural fibres and polypropylene," *Thermochim. Acta*. 337(1-2), 169-177.

Wu, C. N., Saito, T., Fujisawa, S., Fukuzumi, H., and Isogai, A. (2012). "Ultrastrong and high gas-barrier nanocellulose/clay-layered composites," *Biomacromolecules* 13, 1927-1932.

Article submitted: June 24, 2013; Peer review completed: August 26, 2013; Revised version received: September 3, 2013; Accepted: September 15, 2013; Published: September 24, 2013.